

MIT Open Access Articles

The oblique orbit of the super-Neptune HAT-P-11b

The MIT Faculty has made this article openly available. **Please share** how this access benefits you. Your story matters.

Citation: Winn, Joshua N. et al. "The oblique orbit of the super-Neptune HAT-P-11b." *Astrophysical Journal Letters* 723.2 (2010): L223.

As Published: <http://dx.doi.org/10.1088/2041-8205/723/2/L223>

Publisher: IOP Publishing

Persistent URL: <http://hdl.handle.net/1721.1/61779>

Version: Author's final manuscript: final author's manuscript post peer review, without publisher's formatting or copy editing

Terms of use: Creative Commons Attribution-Noncommercial-Share Alike 3.0



THE OBLIQUE ORBIT OF THE SUPER-NEPTUNE HAT-P-11b

JOSHUA N. WINN¹, JOHN ASHER JOHNSON², ANDREW W. HOWARD^{3,4}, GEOFFREY W. MARCY⁴, HOWARD ISAACSON⁴, AVI SHPORER^{5,6}, GÁSPÁR Á. BAKOS⁷, JOEL D. HARTMAN⁷, SIMON ALBRECHT¹

Received 2010 September 8; accepted 2010 September 27

ABSTRACT

We find the orbit of the Neptune-sized exoplanet HAT-P-11b to be highly inclined relative to the equatorial plane of its host star. This conclusion is based on spectroscopic observations of two transits, which allowed the Rossiter-McLaughlin effect to be detected with an amplitude of 1.5 m s^{-1} . The sky-projected obliquity is 103^{+26}_{-10} degrees. This is the smallest exoplanet for which spin-orbit alignment has been measured. The result favors a migration scenario involving few-body interactions followed by tidal dissipation. This finding also conforms with the pattern that the systems with the weakest tidal interactions have the widest spread in obliquities. We predict that the high obliquity of HAT-P-11 will be manifest in transit light curves from the *Kepler* spacecraft: starspot-crossing anomalies will recur at most once per stellar rotation period, rather than once per orbital period as they would for a well-aligned system.

Subject headings: planetary systems — planets and satellites: formation — planet-star interactions — stars: rotation

1. INTRODUCTION

The origin of close-in planets is the longest-standing problem in exoplanetary science (Mayor & Queloz 1995). Recently, the orbits of some close-in planets were found to be highly inclined relative to the equatorial planes of their host stars (see, e.g., Hébrard et al. 2008, Narita et al. 2009, Winn et al. 2009, Triaud et al. 2010). This evidence supports theories for close-in planets in which their orbits shrink due to gravitational perturbations from other bodies followed by tidal dissipation (Matsumura et al. 2010). The evidence disfavors the other leading theory, in which the orbits shrink due to gradual interactions with the protoplanetary gas disk, unless the disks were somehow misaligned with their host stars (Bate et al. 2010, Lai et al. 2010).

To this point, spin-orbit alignment has been measured only for “hot Jupiters,” with masses ranging from $0.4\text{--}20 M_{\text{Jup}}$. We would like to extend these studies to smaller planets, in order to see whether they migrate in a similar way as larger planets, and to understand which factors are associated with orbital misalignment. It has been claimed, for example, that tilted orbits are more prevalent for massive planets (Johnson et al. 2009, Hébrard et al. 2010), or for stars with thinner convection zones (Winn et al. 2010, Schlaufman 2010).

Here we present a spin-orbit study of HAT-P-11b, a “hot Neptune” of mass $0.08 M_{\text{Jup}}$ and radius $0.42 R_{\text{Jup}}$ on an eccentric, 4.9-day orbit around a K4 dwarf (Bakos et al. 2010; B10 hereafter). We observed the Rossiter-McLaughlin (RM) effect (§ 2), and modeled it (§ 3), finding the orbit and stellar spin to be misaligned (§ 4).

2. OBSERVATIONS AND DATA REDUCTION

We obtained 132 new spectra of HAT-P-11 with the High Resolution Spectrograph (HIRES; Vogt et al. 1994) on the Keck I 10m telescope. Most of the new spectra were gathered on nights when transits were predicted. On 2009 Aug 2/3 we gathered 7 spectra during a transit, although fog prevented us from observing before or after the transit. On 2010 May 26/27 we obtained 32 spectra starting at around first contact and extending for a few hours beyond the transit. On 2010 Aug 22/23 we obtained 70 spectra spanning the entire transit and a few hours beforehand and afterward. The remaining 23 spectra were obtained sporadically throughout the 2009–2010 observing season.

We used the instrument settings and observing procedures that are standard for the California Planet Search (Howard et al. 2009). In particular, we used an iodine gas absorption cell to track the instrumental response and wavelength scale. The radial velocity (RV) of each spectrum was measured with respect to an iodine-free template spectrum, using a descendant of the algorithm of Butler et al. (2006). Measurement errors were estimated from the scatter among the fits to individual spectral segments spanning a few Angstroms. Table 1 gives all the Keck/HIRES RVs, including re-reductions of the 50 spectra presented by B10.

3. ANALYSIS

Merging all the RVs into a single analysis requires some care because the host star is chromospherically active. B10 found a photometric signal with period 29.2 days and amplitude 3 mmag, which they attributed to starspots being carried around by stellar rotation. One would expect a corresponding RV signal at the same period and its harmonics, with an amplitude of order 0.3% of the projected stellar rotation speed ($v \sin i_*$), or approximately 5 m s^{-1} . Indeed, B10 found evidence for “stellar jitter” of amplitude 5 m s^{-1} , supporting this interpretation.

We investigated this issue by fitting the out-of-transit RVs with a model consisting of a single Keplerian orbit plus a con-

¹ Department of Physics, and Kavli Institute for Astrophysics and Space Research, Massachusetts Institute of Technology, Cambridge, MA 02139

² Department of Astrophysics, and NASA Exoplanet Science Institute, California Institute of Technology, MC 249-17, Pasadena, CA 91125

³ Department of Astronomy, University of California, Mail Code 3411, Berkeley, CA 94720

⁴ Townes Postdoctoral Fellow, Space Sciences Laboratory, University of California, Berkeley, CA 94720

⁵ Las Cumbres Observatory Global Telescope Network, 6740 Cortona Drive, Suite 102, Santa Barbara, CA 93117

⁶ Harvard-Smithsonian Center for Astrophysics, 60 Garden St., Cambridge, MA 02138

stant acceleration⁷, and seeking evidence for time-correlated residuals. As seen in Figure 1, the residuals are strongly correlated on timescales shorter than 5–10 days, as expected. On longer timescales there are no obvious correlations.

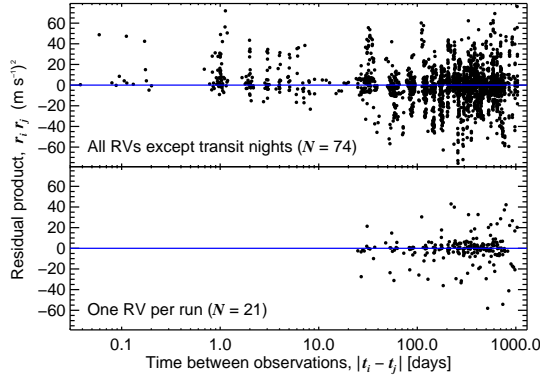


FIG. 1.— **Correlations of the RV residuals.** *Top.*—Products of pairs of residuals, as a function of the time elapsed between the observations. Significant positive correlations are seen for $\Delta t \lesssim 5$ days. *Bottom.*—Same, but restricting the analysis to only one data point per observing run, giving a minimum time separation of 20 days. No significant correlations are seen.

While it would be possible to model the RV covariances, we chose the simpler approach of selecting a subset of RVs that are effectively independent. Specifically, we chose a single spectrum from each observing run, resulting in a sample of 21 out-of-transit RVs spaced apart by a minimum of 20 days.

We turn now to the transit nights. During a single night, one would expect the rotationally modulated RV signal to act as a nearly constant offset. Therefore, each transit night was assigned a free parameter that shifts all the RVs by a common amount; only the intranight variations were deemed significant. With this approach the data from 2009 Aug 2/3 were rendered useless, because no data were gathered outside of the transit. We omitted those data from further consideration.

Our model for the RVs was the sum of the Keplerian orbital motion, a constant acceleration, the RM effect, and the offsets described above. The fitting statistic was

$$\chi^2 = \sum_{i=1}^{123} \left[\frac{RV_i(\text{obs}) - RV_i(\text{calc})}{\sigma_i} \right]^2 + \left(\frac{BJD_c - 2454605.89132}{0.00032} \right)^2 + \left(\frac{P_{\text{days}} - 4.8878162}{0.0000071} \right)^2 + \left(\frac{T_{\text{days}} - 0.0957}{0.0012} \right)^2 + \left(\frac{\tau_{\text{days}} - 0.0051}{0.0013} \right)^2 + \left(\frac{R_p/R_* - 0.0576}{0.0009} \right)^2 + \left(\frac{R_*/R_{\odot} - 0.752}{0.021} \right)^2 + \left(\frac{v \sin i_* - 1.5 \text{ km s}^{-1}}{1.5 \text{ km s}^{-1}} \right)^2, \quad (1)$$

where the first term is the usual sum of squared residuals, and the other terms represent *a priori* constraints on parameters that were determined more precisely from the larger body of

⁷ The evidence for a constant acceleration (linear velocity trend), and the implied existence of another orbiting body besides HAT-P-11b, were established by B10.

data analyzed by B10. In this expression P_{days} is the orbital period in days, BJD_c is a particular time of inferior conjunction; T_{days} is the time between first and fourth contact; τ_{days} is the time between first and second contact; R_p and R_* are the radii of the planet and star; and $v \sin i_*$ is the star’s sky-projected rotation speed.

Each of the 21 orbital RVs was assigned an error bar σ_i equal to the quadrature sum of the measurement error and a “jitter” of 5.5 m s^{-1} , the value giving $\chi^2 = N_{\text{dof}}$ when the orbital RVs were fitted alone. For the transit-night RVs, the jitter was fixed by the requirement $\chi^2 = N_{\text{dof}}$ when fitting the data from that night along with the orbital RVs. The results were 1.8 and 1.5 m s^{-1} for 2010 May 26/27 and 2010 Aug 22/23, respectively. The relative smallness of these values corroborates our assumption that the activity-induced RV variations occur mainly on longer timescales. A similar contrast between intranight and internight jitter was observed previously for HD 189733, another active K star (Winn et al. 2006).

We modeled the RM effect with the technique described by Winn et al. (2005), finding in this case that a sufficiently accurate description for the RV shift is the product of the loss of light and the RV of the portion of the stellar photosphere beneath the planet. We neglected differential rotation, and took the stellar limb-darkening law to be linear with a coefficient of 0.79 (Claret 2004).

Parameter optimization and error estimation were achieved with a Markov Chain Monte Carlo algorithm, using Gibbs sampling and Metropolis-Hastings stepping. Table 2 gives the results for each parameter, based on the 15.85%, 50%, and 84.15% confidence levels of the marginalized *a posteriori* distributions. Figure 2 shows the RV data: the left panel shows the orbital RVs; and the right panel shows the transit-night RVs after subtracting the calculated variation due to orbital motion, thereby isolating the “anomalous RV” due to the RM effect. Figure 3 shows the *a posteriori* distributions for the key parameters $v \sin i_*$ and λ (the sky position angle from the stellar north pole to the orbital north pole).

The most important result is $\lambda = 103_{-10}^{+26}$ degrees, indicating a major misalignment between the stellar rotation axis and the orbit normal. Qualitatively this follows from the observation that the RM effect was observed to be a blueshift throughout the transit, as opposed to the “red-then-blue” pattern of a well-aligned system.

4. DISCUSSION

Because the signal has an amplitude of only 1.5 m s^{-1} , smaller than any other RM signal yet reported, it is important to test the robustness of the results. First, we tried analyzing each transit individually, rather than combining the data from both transits. As shown in Figure 3, the results are in good agreement.⁸ Second, we repeated the analysis without the *a priori* constraint on $v \sin i_*$, the other parameter of greatest relevance to the RM effect. The results were $v \sin i_* = 1.13_{-0.70}^{+2.44} \text{ km s}^{-1}$ and $\lambda = 100_{-9}^{+28}$ degrees. Third, we checked for any correlations between the RM signal and the strength of Ca II H and K emission, or the shape parameters of the instrumental line spread function. Significant correlations would have raised suspicion of systematic errors, but none were found.

⁸ In fact there are three mutually reinforcing datasets: Hirano et al. have submitted a paper reporting $\lambda = 103_{-9}^{+23}$ degrees, based on independent observations of HAT-P-11b (T. Hirano and N. Narita, private communication).

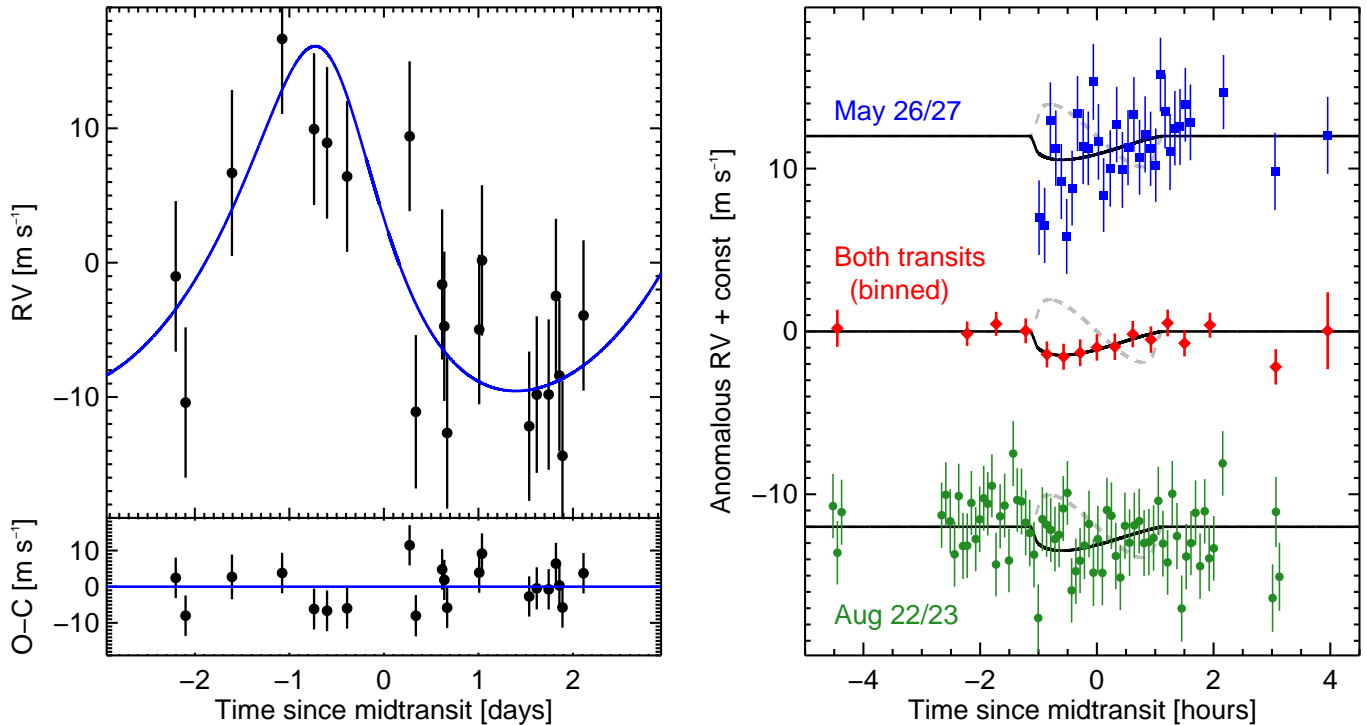


FIG. 2.— **Radial velocities and the RM effect.** *Left.*—Spectroscopic orbit of HAT-P-11, based on the subset of 21 RVs analyzed here. *Right.*—Anomalous RV of HAT-P-11 spanning two transits (top and bottom), and the time-binned combination (middle; binned $\times 7$ with a maximum bin size of 0.5 hr). The orbital contribution to the RV has been subtracted. The solid line shows the best-fitting model of the RM effect. The dashed curve shows the best-fitting “well-aligned” model ($\lambda = 0$, $v \sin i_* = 1.3 \text{ km s}^{-1}$), which is ruled out with $\Delta\chi^2 = 52.4$.

In addition, if the 29.2 day periodicity detected by B10 is indeed the rotation period, then a powerful test for spin-orbit misalignment is available. If the system were well-aligned we would have $\lambda = 0$ and $i_* \approx 90^\circ$. This would imply

$$v \sin i_* = v = \frac{2\pi R_*}{P_{\text{rot}}} = 1.30 \text{ km s}^{-1}, \quad (2)$$

where we have used $R_* = 0.752 R_\odot$ and $P_{\text{rot}} = 29.2$ days (B10). When refitting the data with these constraints, the minimum χ^2 rises from 111.9 to 164.3 ($\Delta\chi^2 = 52.4$), with 114 degrees of freedom. Thus the well-aligned model is ruled out with 7.2σ confidence: either λ is large, or else i_* must be far from 90° to be compatible with the low amplitude of the RM signal. The best-fitting well-aligned model is illustrated with a gray dashed curve in Figure 3.

HAT-P-11b is the first “hot Neptune” for which the RM effect has been measured. Our results suggest that tilted orbits are common for hot Neptunes, just as has been found for hot Jupiters. The same migration mechanisms that are invoked to explain the larger planets with tilted orbits—gravitational scattering by planets, or the three-body Kozai effect—may also have operated in this case. It should be noted that the spin-orbit results are not the only evidence for a perturbative origin for many close-in planets. Further evidence comes from their occasionally high orbital eccentricities, the clustering of their orbital distances near the value expected from tidal circularization, and their tendency to lack companions with periods between 10–100 days (Matsumura et al. 2010).

Since HAT-P-11b is the lowest-mass planet yet probed by RM measurements, and it is misaligned, our findings are at odds with the hypothesis that misalignments occur mainly for

the most massive planets (Johnson et al. 2009). They do, however, support the correlation between large obliquity and orbital eccentricity (Johnson et al. 2009, Hébrard et al. 2010), as the orbit of HAT-P-11b has a significant eccentricity.

Another emerging trend is that misalignments occur mainly for stars with high effective temperatures or large masses ($T_{\text{eff}} > 6250 \text{ K}$ or $M_* \gtrsim 1.2 M_\odot$). Winn et al. (2010) speculated that this is due to tidal interactions: cool stars realign with the orbits, but hot stars cannot realign because tidal dissipation is weaker in their thinner outer convection zones. The HAT-P-11 system is an important test case because the star is cool and low-mass, and yet tidal interactions are weak due to the planet’s relatively small size and long period. If stellar temperature or mass are the determinants then one would expect HAT-P-11 to be well-aligned like other cool stars. But if tides are the underlying factor, then HAT-P-11 would be misaligned, as we have observed. Specifically, with reference to Eqn. (2) of Winn et al. (2010), HAT-P-11 experiences even weaker tides than WASP-8, a cool star already known to have a high obliquity.⁹ Thus, HAT-P-11 is a telling exception to the rule that hot stars have high obliquities: it implicates tidal evolution as the reason for low obliquities among cool stars with more massive planets in tighter orbits.

By good fortune, HAT-P-11 is in the field of view of the *Kepler* spacecraft (Borucki et al. 2010). The precise photometric time series will allow the candidate 29.2-day rotation period to be checked. Asteroseismological studies may reveal the stellar mean density, age, inclination, and other param-

⁹ Matsumura et al. (2010) have also argued that tidal dissipation in the HAT-P-11 system would be too weak to realign the star with the orbit, despite the star’s thick outer convective zone.

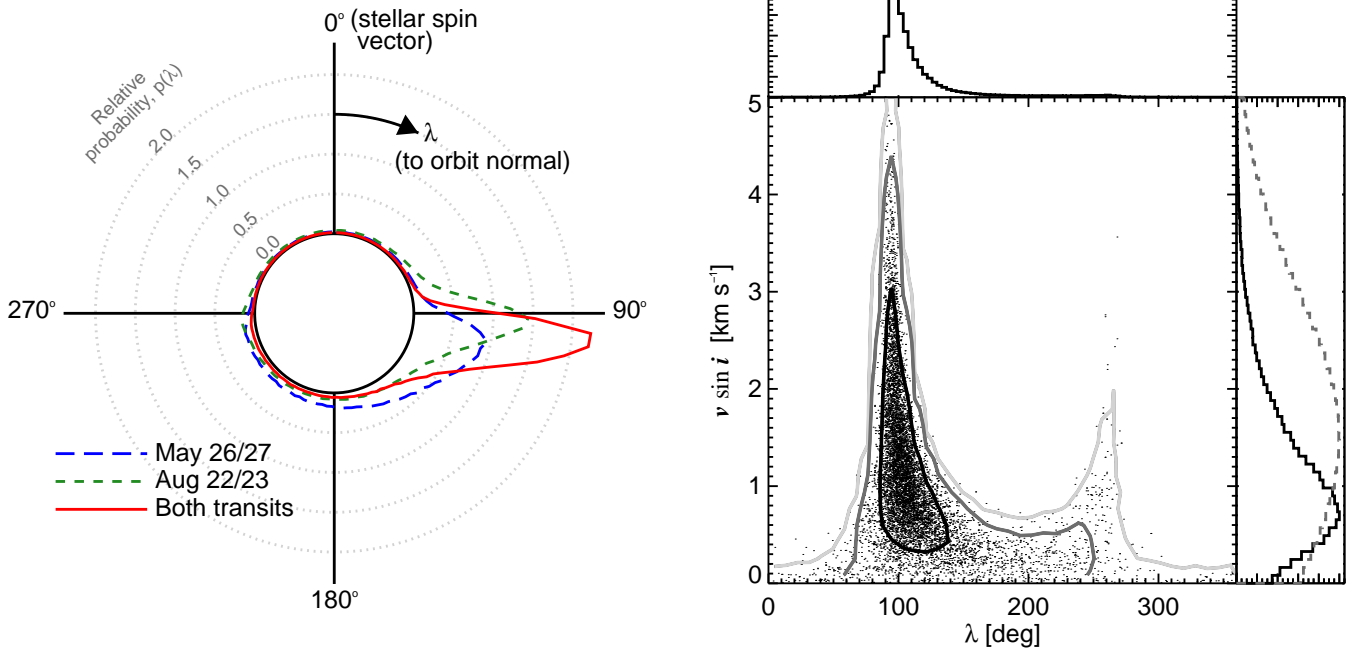


FIG. 3.— **Results for the RM parameters.** *Left.*—In this polar plot, the angular coordinate is λ and the radial coordinate is $p(\lambda)$, the marginalized posterior probability distribution. Results are shown for analyses based only on individual transits, as well as for the entire dataset. *Right.*—Joint constraints on λ and $v \sin i^*$. The contours represent 68%, 95%, and 99.73% confidence limits. The marginalized posterior probability distributions are shown on the sides of the contour plot. The dashed histogram shows the *a priori* constraint on $v \sin i^*$.

ters (Christensen-Dalsgaard et al. 2010). Furthermore we predict that *Kepler* will see a pattern of anomalies in the transit light curves that will betray the system’s spin-orbit misalignment. As usual for a spotted star, there will be a “bump” or “rebrightening” in the transit light curve whenever the planet occults a starspot (see, e.g., Rabus et al. 2009). For a well-aligned star, the bumps recur in successive transits for as long as the spot is on the visible hemisphere. There is a steady advance in phase of the bumps due to the star’s rotation between transits. However, for a star like HAT-P-11 with $\lambda \approx 90^\circ$, the events will *not* recur in this manner, because the star’s rotation moves the spot away from the transit chord. A spot must complete a full rotation before returning to the transit chord, and even then, the planet will miss it unless it has also completed an integral number of orbits.

For HAT-P-11, it happens that $P_{\text{rot}}/P_{\text{orb}} \approx 6$. If the star were well-aligned and had one spot initially on the transit chord, then we would typically see an alternation between 2–3 light curves with bumps, and 2–3 without bumps (when the spot is on the far side). But because of the misalignment, spot

anomalies will only recur every 29.2 days, after the star has rotated once and the planet has completed 6 orbits. Complications may arise due to differential rotation, as well as the multiplicity and evolution of spot patterns. Nevertheless, this phenomenon should allow for an independent test of spin-orbit misalignment for HAT-P-11 as well as other spotted stars.

We thank Norio Narita and Teruyuki Hirano for sharing their results prior to publication, and Dan Fabrycky and Scott Gaudi for helpful discussions. We acknowledge the support from the MIT Class of 1942, NASA grants NNX09AD36G and NNX08AF23G, and NSF grant AST-0702843.

The data presented herein were obtained at the W. M. Keck Observatory, which is operated as a scientific partnership among the California Institute of Technology, the University of California, and NASA, and was made possible by the generous financial support of the W. M. Keck Foundation. We extend special thanks to those of Hawaiian ancestry on whose sacred mountain of Mauna Kea we are privileged to be guests.

REFERENCES

- Bakos, G. Á., et al. 2010, *ApJ*, 710, 1724 (B10)
 Bate, M. R., Lodato, G., & Pringle, J. E. 2010, *MNRAS*, 401, 1505
 Borucki, W. J., et al. 2010, *Science*, 327, 977
 Butler, R. P., Marcy, G. W., Williams, E., McCarthy, C., Dosanji, P., & Vogt, S. S. 1996, *PASP*, 108, 500
 Christensen-Dalsgaard, J., et al. 2010, *ApJ*, 713, L164
 Claret, A. 2004, *A&A*, 428, 1001
 Hébrard, G., et al. 2008, *A&A*, 488, 763
 Hébrard, G., et al. 2010, *A&A*, 516, A95
 Howard, A. W., et al. 2009, *ApJ*, 696, 75
 Johnson, J. A., Winn, J. N., Albrecht, S., Howard, A. W., Marcy, G. W., & Gazak, J. Z. 2009, *PASP*, 121, 1104
 Lai, D., Foucart, F., & Lin, D. N. C. 2010, arXiv:1008.3148
 Mayor, M., & Queloz, D. 1995, *Nature*, 378, 355
 Matsumura, S., Peale, S. J., & Rasio, F. A. 2010, arXiv:1007.4785
 Narita, N., Sato, B., Hirano, T., & Tamura, M. 2009, *PASJ*, 61, L35
 Rabus, M., et al. 2009, *A&A*, 494, 391
 Schlaufman, K. C. 2010, *ApJ*, 719, 602
 Triard, A. H. M. J., et al. 2010, *A&A*, in press [arXiv:1008.2353]
 Vogt, S. S., et al. 1994, *Proc. SPIE*, 2198, 362
 Winn, J. N., et al. 2005, *ApJ*, 631, 1215
 Winn, J. N., et al. 2006, *ApJ*, 653, L69
 Winn, J. N., Johnson, J. A., Albrecht, S., Howard, A. W., Marcy, G. W., Crossfield, I. J., & Holman, M. J. 2009, *ApJ*, 703, L99
 Winn, J. N., Fabrycky, D., Albrecht, S., & Johnson, J. A. 2010, *ApJ*, 718, L145

TABLE 1
RELATIVE RADIAL VELOCITY MEASUREMENTS OF HAT-P-11

BJD _{UTC}	RV [m s ⁻¹]	Error [m s ⁻¹]
2454335.89332	-1.33	1.01
2454335.89998	-2.66	1.03
2454336.74876	-1.30	0.90
2454336.86163	-4.74	1.02
2454336.94961	-7.56	0.94

NOTE. — The RV was measured relative to an arbitrary template spectrum; only the differences are significant. The uncertainty given in Column 3 is the internal error only and does not account for any possible “stellar jitter.” (We intend for this table to be available in its entirety in a machine-readable form in the online journal. A portion is shown here for guidance regarding its form and content.)

TABLE 2
MODEL PARAMETERS

Parameter	Value
<i>Parameters controlled mainly by priors</i>	
Orbital period, P [days]	4.88781501 ± 0.0000068
Midtransit time [BJD _{UTC}]	$2,454,605.89130 \pm 0.00032$
Planet-to-star radius ratio, R_p/R_*	0.0576 ± 0.00090
Orbital inclination, i [deg]	$89.17^{+0.46}_{-0.60}$
Fractional stellar radius, R_*/a	0.0673 ± 0.0018
<i>Parameters controlled mainly by RV data</i>	
Velocity semiamplitude, K [m s ⁻¹]	12.9 ± 1.4
$e \cos \omega$	0.261 ± 0.082
$e \sin \omega$	0.085 ± 0.043
RV offset, 2010 May 26/27 [m s ⁻¹]	-19.8 ± 3.9
RV offset, 2010 Aug 22/23 [m s ⁻¹]	-17.5 ± 4.2
RV offset, all other data [m s ⁻¹]	-13.0 ± 2.2
RV trend, $\dot{\gamma}$ [m s ⁻¹ day ⁻¹]	0.0185 ± 0.0036
Projected stellar rotation rate, $v \sin i_*$ [km s ⁻¹]	$1.00^{+0.95}_{-0.56}$
Projected spin-orbit angle, λ [deg]	103^{+26}_{-10}